Destruction Mechanism of Clay-Covered Karst Collapse

Jiayi Tian[1,a],Yan Gao[1,2,b*]

[1] School of Earth Sciences and Engineering, Sun Yat-sen University, Zhuhai, Guangdong, China

[2] Southern Marine Science and Engineering Guangdong Laboratory (Zhuhai), Zhuhai, Guangdong, China

[a]tianjy25@mail2.sysu.edu.cn, [b]gaoyan25@mail.sysu.edu.cn

Abstract. Based on actual engineering geological data in Guangzhou, this study establishes a finite element numerical model for the clay-covered karst collapse. The coupled Euler-Lagrange method (CEL) is adopted to simulate the process of the clay-covered karst collapse. Multiple sets of numerical simulations are conducted using the orthogonal experimental method. By comparing the numerical simulation results of different cavity spans and friction angles of cohesive soil, the development mode of the clay-covered karst collapse is studied. The mechanism of the clay-covered karst collapse is explained, i.e., after the failure of the soil arch, if the span of the soil arch is too large and causes excessive weight of the overlying soil, the new soil arch cannot withstand the gravitational load of the upper soil, leading to further development into complete collapse; if the cavity span is small, it is more likely for soil to form a stable new soil arch and prevent complete collapse.

Keywords: Karst collapse; Cohesive soil stratum; Destruction mechanism

1 Introduction

The occurrence of ground collapse accidents is usually attributed to adverse geological conditions and weak soil formation, gradually leading to the formation of cavities or loose soil. These conditions further evolve and develop under the influence of loads, rainfall, underground pipeline leakage, and other factors, eventually triggering ground collapse accidents (Wu 2018)[1]. In Guangzhou city, ground collapses can be mainly classified into three types: karst ground collapses, collapses in coal mining subsidence areas, and other collapses, accounting for 97.9%, 0.8%, and 1.3% respectively in the total collapse accidents (Lyu 2020)[2]. It is evident that the collapses in Guangzhou city are predominantly caused by karst geology, with the karst collapse in the overlying stratum being the primary form. The fractures and cavities developed in karst geology provide space for soil displacement, and when coupled with other factors such as groundwater level fluctuations, they easily lead to ground collapse incidents (Dong 2015) [3].

Q. Gao et al. (eds.), *Proceedings of the 2024 7th International Conference on Structural Engineering and Industrial Architecture (ICSEIA 2024)*, Atlantis Highlights in Engineering 30,
https://doi.org/10.2991/978-94-6463-429-7_4

The development of soil cavities in karst areas and other adverse geological conditions provide favorable conditions for the development of ground collapse disasters (Jia 2021) [4]. In terms of the dynamic research on the development of clay-covered karst collapse, two widely recognized theories are the "sub-erosion theory" proposed by Soviet karst geologist A.P. Baplov (1898) and the "vacuum suction erosion theory" proposed by Xu Weiguo and Zhao Guirong (1986) [5]. These two theories can well explain the mechanisms that trigger the movement of soil and explain the phenomena of expansion in soil cavities (Jiang 2017) [6]. Kudai et al. (2021) [7] summarized coastal karst collapse into three processes: subsurface erosion of soil, cavity formation and soil collapse. Luo (2015) [8] summarized that the collapses of cohesive soil are mostly "soil cavity collapses". However, existing studies still lack a systematic investigation of the destruction mechanism of ground collapse. In this study, the Coupled Eulerian-Lagrangian (CEL) method is adopted, which not only enables more accurate calculation of the displacement and the stress of soil but also ensures the convergence of calculation results when the model undergoes large deformation (JEONG 2019) [9]. This further reveals the evolutionary mode and mechanism of the disaster chain in ground collapse and provides a more reasonable and scientific basis for collapse assessment in engineering practice.

2 Numerical simulation modeling

Taking Guangzhou as the representative, where cohesive soil stratums are relatively extensive (Meng 2020) [10], finite element simulations are conducted by ABAQUS. The bottom is consisted of a 5m thick karst stratum, while the uppermost layer is the artificial fill to simulate the impact of surface engineering activities. The thickness of the fill stratum is 0.5m and the corresponding gravitational load is 10kPa. The density, elastic modulus, and Poisson's ratio of the artificial fill are 1960 kg/m^3, 26.6 MPa, and 0.3, respectively. Only the gravitational load of the fill stratum is considered as the external load. The middle layer represents the cohesive soil stratum, which is composed of typical silty clay commonly encountered in engineering projects in Guangzhou. The density, elastic modulus, and Poisson's ratio of the cohesive soil are 1840 kg/m^3, 40.0 MPa, and 0.3, respectively. The natural height of cohesive soil cavities in Guangzhou generally ranges from 0.5m to 4m (corresponding to diameters of semi-circular cavities from 1m to 8m). Therefore, the basic value of the cavity diameter is set to 5m. To minimize boundary effects, the width of the soil stratum is set to 40m, and rigid boundaries with a width of 1m are placed on both sides. Large deformations are achieved in the finite element analysis by adopting the Coupled Eulerian-Lagrangian method. The Mohr-Coulomb criterion is employed to represent the soil yield criteria during the numerical simulation. The friction angle of the cohesive soil ranges from 13° to 30°, within the conventional range of values.

3 Characterization of clay-covered karst collapse

As shown in Figure 1, the development of the plastic zone, collapse process, maximum surface displacement and subsidence rate of the soil with a cavity diameter of 5m are influenced by the increasing friction angle of the cohesive soil. With the passage of time, the plastic zone gradually extends, and the displacement increases. However, no ground collapse occurs, eventually leading to the formation of a stable soil arch. As the friction angle of the cohesive soil increases, the arching effect of the soil becomes more stable, resulting in a smaller extent of plastic zone expansion, reduced surface settlement, and the formation of a larger stable soil arch.

To explore the different collapse modes associated with smaller and larger cavity diameters, this study further investigates the collapse development process for a larger cavity diameter of 6m, as shown in Figure 2. With the passage of time, the plastic zone gradually extends and the displacement increases. The collapse rate stabilizes, followed by further expansion of the plastic zone and a rapid increase in the collapse rate until complete collapse occurs. As the friction angle of the cohesive soil increases, the arching effect of the soil becomes more stable, resulting in a smaller extent of plastic zone expansion and minimal surface settlement. When the friction angle is within the range of 24° to 26°, the soil reaches a state of limit equilibrium. If the friction angle is smaller than this value, the soil gradually progresses towards complete collapse, whereas if it is higher than this value, the surface settlement is negligible.

It can be observed that the development of ground collapse is related to the span of the natural soil cavity. Smaller span cavities are more likely to form new stable soil arches during the collapse process, thereby avoiding further collapse. On the other hand, larger span cavities are less likely to form new soil arch structures during the collapse process. Once the arching effect is disrupted, it inevitably leads to a complete collapse of the covering layer. In the risk assessment of karst collapse, it is evident that the larger the span of the cavity, the higher the risk of collapse (Yuan 2022) [11].

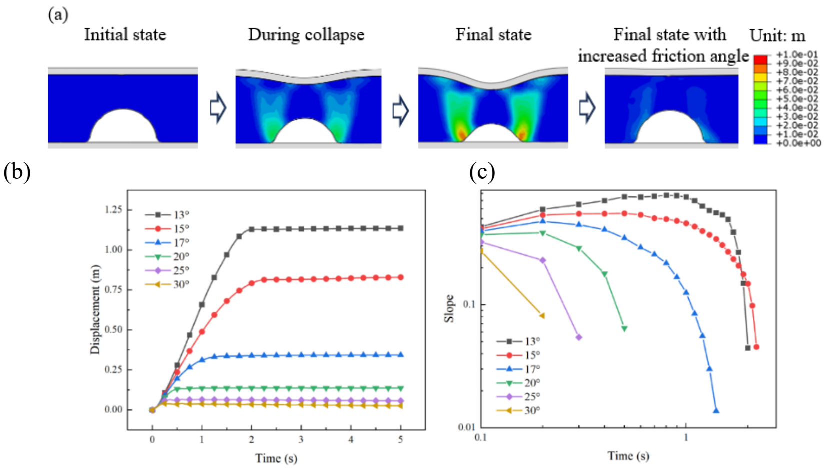

Fig. 1. Influence of friction angle on ground collapse with cavity diameter of 5m: (a) development of plastic zone; (b) maximum surface displacement; (c) collapse rate

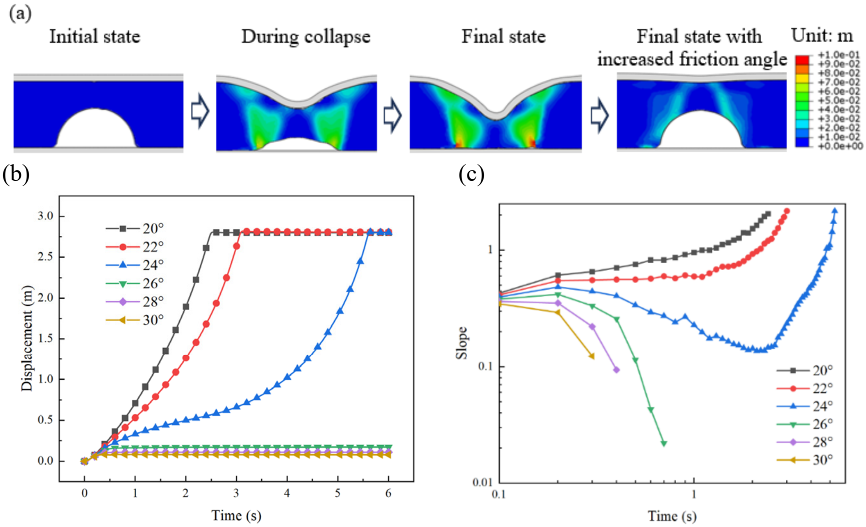

Fig. 2. Influence of friction angle on ground collapse with cavity diameter of 6m: (a) development of plastic zone; (b) maximum surface displacement; (c) collapse rate

The development of the overlying cohesive soil cavity is related to the diameter of the natural soil cavity. There are two different collapse modes observed when the cavity diameter is relatively large or small. A cavity diameter of 6m and 5m is selected to represent the cases of large and small cavity diameters, respectively. As shown in Figure 3, the dashed line represents the variation of the soil arch at different stages of ground collapse. By comparing the collapse curves, it can be observed that when the cavity diameter is large, the soil undergoes plastic failure at the foot of the arch (as indicated by the point in Figure 3) after being influenced by external factors. The arch effect subsequently fails, and the surrounding soil compresses and moves towards the location of arch failure. Due to the large span between the two failure points of the arch, the new arch structure cannot withstand the gravitational load of the overlying soil mass, resulting in complete collapse. On the other hand, when the cavity diameter is small, the surrounding soil compresses and moves towards the location of arch failure after the arch collapses. However, due to the smaller span between the failure points, the newly formed arch structure can still bear a relatively small gravitational load from the overlying soil, ultimately forming new small arches and reaching a stable state without experiencing complete collapse.

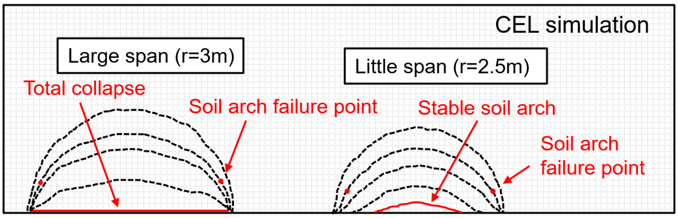

Fig. 3. Comparison of collapse patterns for large and small soil cavity diameters

4 Analysis of the clay-covered karst collapse mechanism

4.1 Soil arch failure mechanisms and influencing factors

Soil arches typically fail at the arch foot. From a mechanical model perspective, if the arch is subjected to distributed loads, failure will first occur near the arch foot, where the central angle measures approximately 54°. (Zhai 2006) [12]. For soil arches, as the burial depth increases, the arch experiences higher earth pressure, causing the failure location to be more biased towards the arch foot. Additionally, the stronger the soil strength, the greater the load and soil pressure it can withstand. The differential earth pressure caused by different burial depths has a relatively smaller influence, so the failure angle of the soil arch under distributed loads will be more biased towards 54°, which represents the failure angle of the arch structure under distributed loads, as shown in Figure 4.

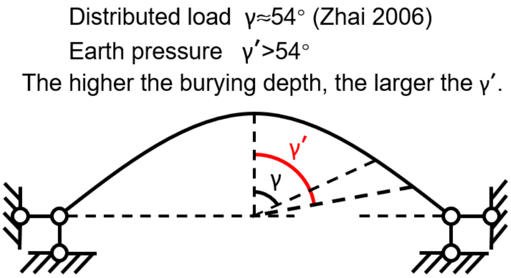

Fig. 4. Soil arch mechanics model

4.2 The development patterns of clay-covered karst collapse

This study compares the results of Jia Long's model test for clay-covered collapse (Jia 2021) [4]. The collapse development curve is shown in Figure 5. The collapse mode progresses as the cohesive soil continuously detaches, resulting in the enlargement of the soil cavity. Eventually, the roof of the cavity becomes too thin, leading to instability and subsequent collapse of the soil. This development process from instability to collapse is consistent with the case discussed earlier, where the cover thickness is 3m, both exhibiting roof instability leading to collapse.

In natural conditions or situations with minimal engineering influence, the triggering factor for clay-covered collapse is typically the thinning of the roof, which leads to a decrease in bearing capacity and eventual instability and collapse. However, in cases where the engineering activities have a significant impact, the triggering factor for collapse is the external load, which often causes collapse before the soil mass reaches its limit size of the soil arch (Luo et al. 2015) [8]. The collapse simulation in this study mainly focuses on collapse induced by external load, except for the case where the cover thickness is 3m, where the triggering factor is roof instability leading to collapse. The development of the plastic zone and the variation in collapse rate also differ significantly from those induced by external load.

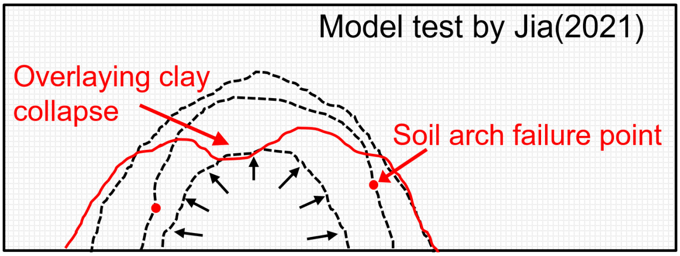

Fig. 5. Experimental collapse curves for modeling clay-covered karst collapse

In terms of the development of the plastic zone, in the case of roof instability leading to collapse, the plastic zone extends from the crown of the arch to the ground surface, resulting in plastic failure and subsequent instability and collapse of the upper part of the soil arch. On the other hand, in the case of collapse induced by external load, the plastic zone gradually develops from the foot of the soil arch towards the ground surface, causing ground subsidence. Regarding the variation in collapse rate, in the case of roof instability leading to collapse, the collapse rate initially develops slowly, followed by a noticeable acceleration after instability until complete collapse. Conversely, in the case of collapse induced by external load, the collapse rate steadily increases until it reaches a constant value, indicating the collapse has reached a stable stage.

This study integrates various collapse factors and different failure mechanisms of the soil arch to obtain the development pattern of the clay-covered collapse, as shown in Figure 6. In karst areas, when the natural soil cavities in the cohesive soil cover develop with minimal external influences, the cavities may develop until the roof becomes too thin, leading to instability and subsequent collapse of the upper soil. The simulation in this study for a 3m clay stratum thickness represents this mode of failure. However, when the cavities are greatly influenced by external factors, they may collapse before reaching their limit size. Under the action of external loads, the soil arch is disrupted at the foot of the arch, and the soil tends to form a new stable soil arch. If the span of the original soil arch is small (≤5m), the new soil arch will remain stable. If the span of the original soil arch is large (≥6m) or the load is significant, the complete collapse can occur due to either the self-weight of the soil above the arch or excessive external loads.

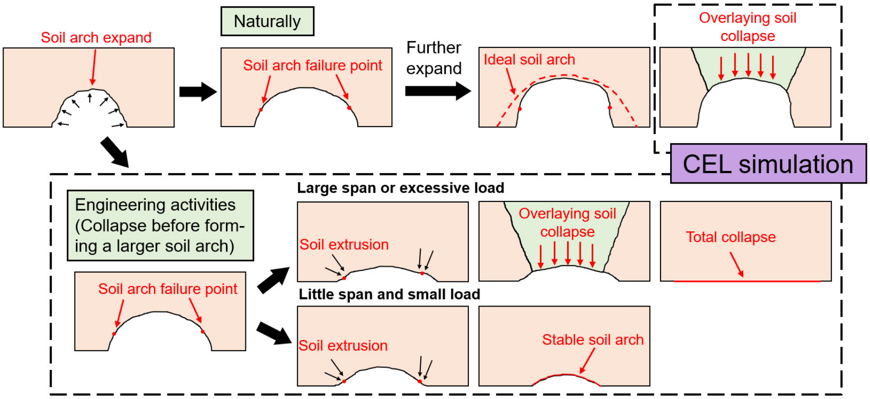

Fig. 6. Development patterns of clay-covered karst collapse.

5 Conclusions

The collapse mode of cohesive soil stratum is investigated through finite element numerical simulations. The results demonstrate that in karst areas, when natural soil cavities are subjected to significant external influences during their formation, the external load disrupts the initially stable soil arch of the cohesive soil stratum. This leads to the displacement of the soil towards the cavity and the formation of smaller soil arches. When the diameter of the natural soil cavity is small, the newly formed soil arch resulting from soil displacement is capable of supporting the gravitational load of the overlying soil and external loads, thereby maintaining to be stable and preventing complete collapse. However, when the span of the natural soil cavity is large, the failure of the soil arch occurs near the arch foot, causing soil displacement primarily at the foot. As a result, the new soil arch cannot withstand the gravitational load of the large-span overlying soil, resulting in instability and complete collapse.

Acknowledgement

The research was supported by National Natural Science Foundation of China (42072295), National Key R&D Program of China (2022YFC3005203), and Guangdong project (2017ZT07Z066).

References

1. WU Y.N., ZHOU S.Z., WANG Y.L., et al. (2018) Summary of karst collapse monitoring methods in China and abroad. J. Shandong Land and Resources, 34(12): 1-6. (in Chinese)
2. Lyu M.N. (2020) Analysis of ground settlement in Guangzhou city in recent years and countermeasures for prevention and control. J. Scientific and technological innovation, (36): 137-138. (in Chinese)

3. Dong H.G. (2015) The formative environment and disaster -inducing factors of ground collapse disaster analysis in the Pearl River Delta of ground collapse. J. Geology and Mineral Resources of South China, 31(3):291 -296. (in Chinese)
4. Jia L. (2021) Early warning and assessment of cover-collapse sinkhole induced by urban construction in karst area—take the Jinshazhou area as an example. D. China University of Geosciences.
5. Xu W.G., Zhao G.R. (1986) On mechanism of karst collapse. J. Journal of Coal Science & Engineering, 02: 1-11.
6. Jiang F.W. (2017) Study on the developing model of karst collapse. J. Carsologica Sinica, 36: 137-138.
7. KUDAI K., SASSA S., YANG S., et al. (2021) Influence of soil and hydraulic conditions on the processes of internal erosion, cavity formation and collapse behind coastal structures. J. Coastal Engineering, 170: 104013.
8. Luo X.J. (2015) Further discussion on mechanism of covered karst ground collapse. J. Journal of Engineering Geology. 23(05): 886-895.
9. JEONG S., LEE K. (2019) Analysis of the impact force of debris flows on a check dam by using a coupled Eulerian-Lagrangian (CEL) method. J. Computers and Geotechnics, 116: 103214. DOI:10.1016/j.compgeo.2019.103214.
10. Meng Y. (2020) Multi-parameter monitoring, early warning and risk prevention of karst collapse in Guanghua Basin. D. China University of Geosciences.
11. Yuan Y.F., Zhang Q., Yan M., et al. (2022) Karst collapse risk assessment based on AHP-EWM-FT. J. Journal of Safety and Environment, 22(06): 2986-2993.
12. Zhai J.Y. (2006) Arched buckling structure damage under semi-cross load. J. Journal of Henan University of Urban Construction, 2006(06): 73-75+80.